

## Physicochemical Studies on Microemulsions. 6. Phase Behavior, Dynamics of Percolation, and Energetics of Droplet Clustering in Water/AOT/*n*-Heptane System Influenced by Additives (Sodium Cholate and Sodium Salicylate)

S. P. Moulik,\* G. C. De, B. B. Bhowmik, and A. K. Panda

Centre for Surface Science, Department of Chemistry, Jadavpur University, Calcutta 700 032, India

Received: February 1, 1999; In Final Form: June 2, 1999

The phase behavior as well as the volume- and temperature-induced percolation of a water in oil (w/o) microemulsion system of water/AOT/*n*-heptane have been studied in detail in the absence and presence of additives, sodium cholate (NaC) and sodium salicylate (NaS). The results have been examined in light of the appropriate scaling equations. The scaling parameters have been observed to be not in agreement with the predicted values. The energetics of droplet clustering leading to percolation have been also estimated. The amphiphile-coated size of the water nanodroplets and their diffusion coefficient and polydispersity have been estimated in the pre- and postpercolation stages. Rationalization of the results has been attempted.

### Introduction

Microemulsions are stable and isotropic dispersions of water in oil (w/o), or vice-versa, stabilized by an amphiphile monolayer.<sup>1–3</sup> The study of their phase behaviors is an important exercise regarding their feasible formation as well as their stability conditions.<sup>4–6</sup> Of the different physical properties of w/o microemulsions, percolation of conductance is striking where a manyfold (100–1000 times) increase in conductance can take place after a threshold volume fraction of the dispersant (water) at a constant temperature or after a threshold temperature at a constant composition.<sup>4,7–11</sup> The enhancement in conductance is considered effective by way of either “hopping” of ions<sup>12–17</sup> from droplet to droplet after a threshold droplet density or ion transfer<sup>18–25</sup> through the nonpolar continuum (oil) by a “transient–fusion–mass transfer–fission” mechanism after a threshold temperature. This area has been intensively studied and quantification with adequate theories has been attempted.<sup>21,24,26–31</sup>

In recent years, effects of additives on conductance percolation have been examined.<sup>20,32–38</sup> The phenomenon has been shown to occur earlier or be delayed in the presence of certain additives; however, many of them may also remain totally ineffective. The compounds hydroxy bile salts (sodium cholate and deoxycholate) have been found to assist percolation by reducing either the threshold volume fraction of water or the threshold temperature, whereas aromatic compounds, viz., toluene, xylene, salicylate, benzene, and naphthalene, have been observed to retard or hinder percolation by increasing the threshold volume fraction or temperature. Probable mechanisms for these effects have been put forward.<sup>17,32–34</sup> It has been suggested that the hydroxy bile salts can form “channels” in the droplet fusion process, thus helping in easier transfer of ions, whereas the aromatic compounds “block” the fusion of droplets,<sup>19,33,34</sup> thus delaying the ion transfer; both explanations apparently rule out the “hopping” mechanism. In a recent work, the “transient–fusion–mass transfer–fission” mechanism has been suggested for the weak and strong conductance at pre- and postpercolation stages in w/o microemulsions consisting

of water/AOT/decane.<sup>39</sup> A nonpercolating w/o microemulsion system of water/AOT/xylene (here the molecules of the oil xylene themselves block the process of fusion) has been shown to exhibit percolation by the presence of a sufficient concentration of the “assister” molecules of sodium cholate.<sup>34</sup> In their detailed investigations on the effects of additives on conductance percolation, Ray, Bisal, and Moulik<sup>33</sup> and Ray, Paul, and Moulik<sup>34</sup> have tested the performance of the scaling equations. A general departure from the expectations has been observed.

It is considered that droplets of water form clusters at the percolation stage, and the clusters can be considered to form a separate phase<sup>33,36,40–42</sup> like a pseudophase of micelles in a surfactant solution at the critical micellar solution, cmc. By determining the threshold temperatures for percolation at different overall concentrations of the dispersed phase for a fixed [water]/[amphiphile] ratio,  $\omega$ , the energetics of the percolation process have been evaluated very recently by Moulik and Ray<sup>40</sup> and Ray, Bisal, and Moulik.<sup>33</sup> This rationale has been also used by Ajith and Rakshit<sup>41</sup> as well as Alexendrakis, Holzwrath, and Hatton<sup>42</sup> and Nazzario, Hatton, and Cresko.<sup>36</sup> Ray, Paul, and Moulik<sup>34</sup> have also estimated the activation energies for percolation in the presence of additives as was done earlier by Mukhopadhyay, Bhattacharya, and Moulik.<sup>20,32</sup>

In this study, we have examined the phase behaviors of the ternary system (water/AOT/*n*-heptane) in the presence and absence of the additives sodium cholate (NaC) and sodium salicylate (NaS) as well as at varied temperatures to essentially locate the mono- and multiphasic regions. On the basis of these findings, an elaborate attempt to understand the conductance percolation of water/AOT/*n*-heptane w/o microemulsion system in the presence of the bile salt (sodium cholate) and the hydrotrope sodium salicylate has been made. The performance of the scaling equations, activation energy for percolation, and energetics of percolation have been assessed. Besides, the droplets' hydrodynamic dimension, polydispersity, and diffusion coefficient at the percolation stage have been determined by the dynamic light-scattering (DLS) method. An attempt has been made to rationalize the results on a physical-chemical basis.

\* Corresponding author. Fax: 91-33-473-4266. E-mail: spmcjsju@cal2.vsnl.net.in.

## Materials and Methods

**Materials.** The AOT (sodium dioctylsulfosuccinate, 99% pure), sodium cholate (NaC), and sodium salicylate (NaS) of AR grade were purchased from Sigma. *n*-Heptane (AR grade) was purchased from S.D. Fine Chemicals, India. They were used as received. All the aqueous solutions were prepared in doubly distilled water of specific conductance  $2\text{--}4\ \mu\text{S cm}^{-1}$  at  $30\ ^\circ\text{C}$ .

**Methods. Phase Formation in Relation to Preparation of Microemulsion.** For phase studies, AOT solutions in *n*-heptane at different concentrations were taken in several stoppered test tubes and they were placed in a constant temperature water bath. To each of these samples, water was added from a microburet under constant stirring condition until the solution became just turbid due to phase separation. To understand the effects of the additives, similar additions of  $0.1\ \text{mol dm}^{-3}$  of NaC and  $1.0\ \text{mol dm}^{-3}$  NaS to the AOT solution in *n*-heptane were made up to the turbidity point. The measurements were checked for reproducibility, and the compositions were expressed in wt % to construct the phase diagrams on triangular coordinates. During the phase study, in addition to low viscous clear and turbid solutions, clear and turbid gels were also observed for several compositions.

For the percolation study, w/o microemulsions were chosen from the low viscous clear monophasic zones which were stable in a wide range of temperature.

**Conductance Measurements.** Conductance measurements (with  $\pm 0.5\%$  accuracy) were taken at a frequency of 1 kHz using a Jenway (England) conductometer in a temperature-compensated dip-type cell of cell constant  $1.08\ \text{cm}^{-1}$  placed in a Neslab RTE-100 temperature-controlled bath of accuracy  $\pm 0.1\ ^\circ\text{C}$ .

For volume-induced percolation measurements, a mixture of AOT and *n*-heptane in the mole ratio 1:16 was taken in a beaker with the cell, and water (or aqueous solution of NaC or NaS) was added in aliquots from a microburet with constant stirring. The conductance was measured at each addition after allowing sufficient time for the attainment of constant temperature. Measurements were taken at five different temperatures.

For temperature-induced percolation, four mole ratios ( $\omega$ ) of [water]/[AOT] were used, and at each  $\omega$ , measurements were taken at four different droplet concentrations. The droplet concentrations were varied by diluting the microemulsion with the oil. In the first set, no additive was used, whereas in the second and third sets, aqueous solutions of  $0.1\ \text{mol dm}^{-3}$  NaC and  $1.0\ \text{mmol dm}^{-3}$  NaS were used, respectively.

**Dynamic Light-Scattering Measurements.** Dynamic light-scattering (DLS) measurements were taken in a dynamic light-scattering spectrophotometer (model DLS-700, Otsuka Electronics Co. Ltd., Japan, fitted with a 5 mW He-Ne laser, operating at 632.8 nm) by placing the sample tube in the temperature-controlled chamber of the goniometer. All measurements were taken at a  $90^\circ$  angle. The autocorrelation function of the scattered intensity was obtained from a 1024-channel photon correlator. The results of measurements for each sample were processed in a computer and the hydrodynamic diameter ( $d_h$ ) of the droplets was obtained from the estimated diffusion coefficient ( $D$ ) and the Stokes-Einstein equation. The polydispersity index (PDI) values were also computed from the scattering results. A PDI value of 0.1 represents monodispersity; values greater than 0.1 indicate polydispersity in the sample.

## Results and Discussion

**Phase Behaviors.** The percolation phenomenon in a w/o microemulsion (water/AOT/*n*-heptane) both in the presence and

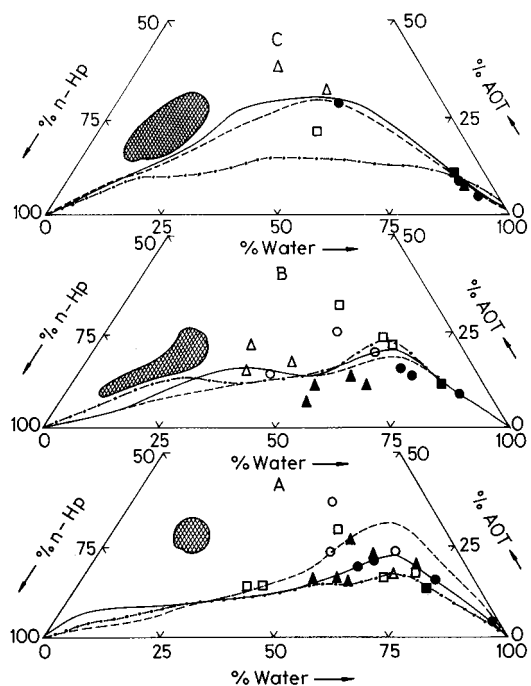


**Figure 1.** Truncated triangular phase diagrams of water/AOT/*n*-heptane system under varied conditions: (A) no additive; (B)  $0.1\ \text{mol dm}^{-3}$  NaC; (C)  $1.0\ \text{mol dm}^{-3}$  NaS. Temperatures (K): (—) 283; (---) 298; (- · -) 323. The boundary curve at each temperature demarcates the single-phase zone (top portion) from the multiphase zone (bottom portion). The studied compositions fall in the shaded enclosures in the diagram. Open symbols ((○) 283 K; (△) 298 K; (□) 323 K) in the monophasic zones represent clear gels. Full symbols ((●) 283 K; (▲) 298 K; (■) 323 K) in the multiphase region represent turbid gels.

absence of additives has been examined with variable water content and temperature. It is thus necessary to simultaneously examine the phase behaviors of the samples in the presence of additives as well as at varied temperatures.

In Figure 1, the triangular coordinated phase diagrams of the studied system without and with NaC and NaS are illustrated in parts A, B, and C. In this diagram, the boundary zones between the single and multiphase compositions are depicted. It is seen in the figure that an increase in temperature from 10 to  $50\ ^\circ\text{C}$  has increased the monophasic zone for all three cases. On the whole, NaC favors formation of the single phase whereas NaS disfavors it compared to the no additive situation. In the absence of additives, the temperature can differentiate the phase formation toward the water end, which shifts toward the middle of the diagram in the presence of NaS, and with NaC there is hardly any difference. Nearly comparable phase diagrams have been reported for water/AOT/*n*-heptane system in the presence of a number of water-soluble polymers as additives.<sup>43</sup>

In the phase studies, several clear and turbid gel-forming states have been observed. These are indicated by open and full symbols in the diagram. A detailed study would realize more such situations and other phase intricacies as well. This is kept pending for not being in line with the objective of the work. It may be mentioned that none of the studied percolating compositions had viscous or gelling consistencies.

The compositions of the studied samples along with the temperature of measurements are presented in Table 1 so that one can readily get them from the locations shown in the diagram (Figure 1) with hatched areas. It is clearly evident that the studied compositions were always in the single-phase zone; their percolation events were not affected by the complexity of multiphase formation. The energetics of percolation (i.e., the

TABLE 1

(A) Temperature-Dependent Composition of Water/AOT/*n*-Heptane System at the Point of Maximum Addition of Water

temp/K	composition (wt %) water/AOT/ <i>n</i> -heptane
No Additive	
30	15:31:54
35	15:30:55
40	15:30:55
45	16:27:57
49	16:26:58
0.1 mol dm <sup>-3</sup> NaC	
30	16:25:59
35	17:22:61
40	17:22:61
45	17:22:61
50	17:22:61
1.0 m mol dm <sup>-3</sup> NaS	
30	32:15:53
35	32:14:54
40	30:15:55
45	29:15:56
49	26:16:58

(B) Composition for Temperature-Induced Percolation of Water/AOT/*n*-Heptane System with Corresponding Threshold Value ( $\theta_i$ ) and the Studied Range

$\omega$	composition (wt %) water/AOT/ <i>n</i> -heptane	temperature range/K
No Additive		
30	20:25:55	308–334
35	19:28:53	309–314
40	16:26:58	303–318
0.1 mol dm <sup>-3</sup> NaC		
25	12:12:76	291–330
30	9:10:81	283–303
35	17:23:60	282–288
40	12:20:68	282–286
1.0 m mol dm <sup>-3</sup> NaS		
30	20:25:55	308–317
35	18:13:69	291–334
40	16:10:74	296–332
45	18:10:72	298–333

energies of activation and clustering) are, therefore, manifestations of fusion dynamics and association extents of the nano-droplets of dispersed AOT-coated water by the influence of either the concentration or the temperature.

**Volume-Induced Percolation.** The dependence of percolation of conductance on the volume fraction ( $\phi_d$ ) of the microdispersed phase (AOT + water) at 303 K with and without NaC is presented in Figure 2. A representative volume-induced percolation of the H<sub>2</sub>O/AOT/*n*-decane system is also presented in the figure for a ready comparison. The threshold volume fraction ( $\phi_d^t$ ) of the dispersed phase required for the onset of percolation was obtained from the maximum in the  $(\delta \ln \sigma / \delta \phi_d)$  vs  $\phi_d$  plot shown in the inset of the figure. The threshold values at different temperatures with corresponding [water]/[AOT] mole ratios ( $\omega$ ) are given in Table 2. From this figure and table, it is observed that  $\phi_d^t$  decreases with increasing temperature. Assuming the water droplets to be spherical and using the relation  $R_W = 0.133\omega$  (nm)<sup>44</sup> ( $R_W$  is the radius of the spherical water pool), the number of water droplets ( $N_d$ ) at the percolation threshold was calculated. The results are also presented in Table 2. The number of droplets increases as  $\phi_d^t$  decreases with increasing temperature. It is normally considered that the amphiphiles are accommodated on the droplet surface. To satisfy this rationale, for a constant [AOT] in the ternary mixture, finer

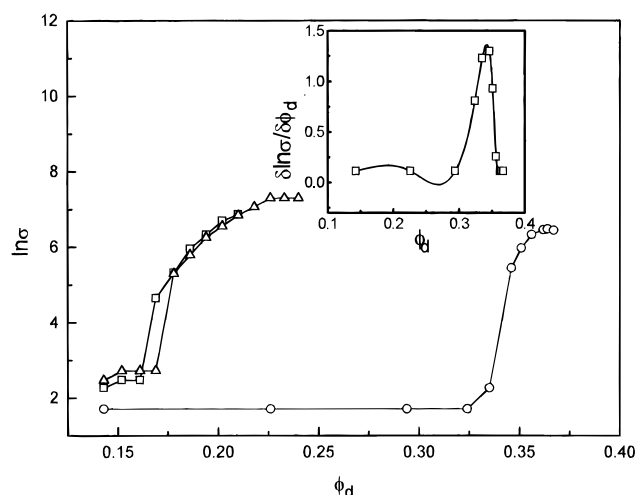


Figure 2. Volume-induced percolation of conductance of w/o microemulsion at 303 K in the absence and presence of additives: (O) no additive (H<sub>2</sub>O/AOT/*n*-heptane system); (Δ) 0.1 mol dm<sup>-3</sup> NaC (H<sub>2</sub>O/AOT/*n*-heptane system); (□) no additive (H<sub>2</sub>O/AOT/*n*-decane system). Inset: differential plot for the first system.

TABLE 2: Scaling Law Parameters for Water-Induced Percolation of Water/AOT/*n*-Heptane Microemulsion System in the Absence and Presence of NaC at Different Temperatures

temp/K	$\phi_d^t$	$N_d \times 10^{-18}$	$\ln k$	$m$	corr. coeff.
System I: 1.5 g AOT + 8.0 mL <i>n</i> -Heptane + Water					
303	0.33	1.35	$16.20 \pm 0.58$	$2.62 \pm 0.12$	0.999
308	0.32	2.00	$11.36 \pm 0.11$	$1.28 \pm 0.03$	0.999
313	0.31	2.25	$10.40 \pm 0.25$	$0.96 \pm 0.07$	0.995
318	0.27	4.18	$12.22 \pm 0.03$	$1.63 \pm 0.01$	0.999
322	0.25	5.14	$12.96 \pm 0.49$	$1.83 \pm 0.15$	0.993
System II: 1.5 g AOT + 8.0 mL <i>n</i> -Heptane + 0.1 mol dm <sup>-3</sup> Aqueous NaC					
303	0.26	8.16	$9.66 \pm 0.20$	$0.67 \pm 0.05$	0.992
308	0.25	10.69	$10.26 \pm 0.16$	$0.81 \pm 0.04$	0.996
313	0.22	14.44	$12.38 \pm 0.19$	$1.68 \pm 0.06$	0.997
318	0.21	20.44	$12.95 \pm 0.42$	$1.91 \pm 0.14$	0.992
322	0.20	24.81	$11.88 \pm 0.44$	$1.60 \pm 0.15$	0.983

droplet dispersion with increasing number should arise with decreasing dispersant (water) volume, i.e., with decreasing  $\phi_d^t$ . It is also evident from the table that in the presence of 0.1 mol dm<sup>-3</sup> NaC,  $\phi_d^t$  is lowered; NaC thus assists percolation.

**Temperature-Induced Percolation.** Temperature-induced percolation of the microemulsion system was studied at different  $\omega$  values. At each  $\omega$ , the threshold temperature of percolation ( $\theta_i$ ) was determined for four different droplet concentrations with and without NaC and NaS from the  $(\delta \ln \sigma / \delta \theta)$  vs  $\theta$  plots shown in the inset of Figure 3 wherein the general nature of temperature percolation is illustrated. The  $\theta_i$  values as a function of  $\omega$  are given in Table 3. It is evident from Table 3 that  $\theta_i$  decreases with  $\omega$ ; the bigger droplets favorably combine to transfer ions to augment percolation. The phenomenon is initiated at lower temperature by NaC and is extended to higher temperature by NaS.

**Performance of Scaling Equations.** At constant temperature in the postpercolation stage, the water-induced percolation usually obeys the scaling law<sup>27–29</sup>

$$\sigma = k(\phi_d - \phi_d^t)^m \quad (1)$$

where  $\sigma$  is the conductance of the microemulsion system and  $k$  is a constant related to the conductance of the dispersed phase. The theoretical value of the exponent  $m$  is 1.9 for both “static”



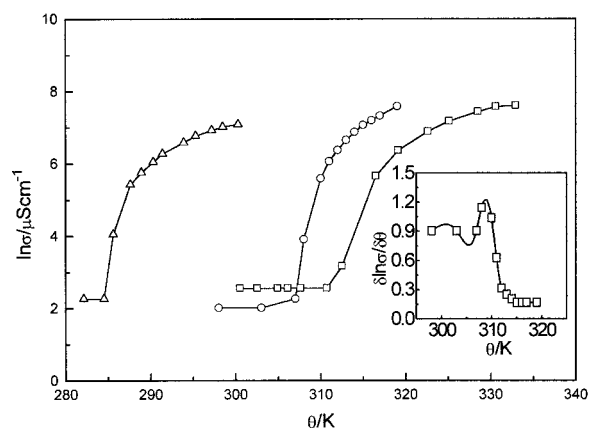


**Figure 3.** Temperature-induced percolation of conductance of H<sub>2</sub>O/AOT/*n*-heptane w/o microemulsion system [composition: H<sub>2</sub>O/AOT/*n*-heptane 1:0.63:2.28 (w/w);  $\omega = 39.52$ ]: (○) no additive; (△) 0.1 mol dm<sup>-3</sup> NaC; (□) 1.0 mol dm<sup>-3</sup> NaS. Inset: differential plot for the first system.

**TABLE 3: Scaling Law Parameters for Temperature-Induced Percolation of Water/AOT/*n*-Heptane Microemulsion System in the Absence and Presence of Additives at Different  $\omega$**

$\omega$	$\theta/k$	$\ln P$	$n$	corr.coeff.
No Additive: 1.5 g AOT + 8.0 mL <i>n</i> -Heptane + Water				
30	316	$2.91 \pm 0.10$	$1.56 \pm 0.04$	0.999
35	313	$5.09 \pm 0.02$	$0.99 \pm 0.01$	0.996
40	308	$4.79 \pm 0.01$	$1.16 \pm 0.01$	0.999
45	309	$6.54 \pm 0.00$	$0.52 \pm 0.00$	1.000
With 0.1 mol dm <sup>-3</sup> NaC:				
1.5 g AOT + 8.0 mL <i>n</i> -Heptane + 0.1 mol dm <sup>-3</sup> NaC				
25	298	$4.38 \pm 0.01$	$1.02 \pm 0.01$	0.999
30	294	$4.51 \pm 0.02$	$0.98 \pm 0.01$	0.999
35	290	$2.20 \pm 0.16$	$1.09 \pm 0.05$	0.997
40	287	$5.12 \pm 0.03$	$0.78 \pm 0.02$	0.999
With 1.0 mmol dm <sup>-3</sup> NaS:				
1.5 g AOT + 8.0 mL <i>n</i> -Heptane + 1.0 mol dm <sup>-3</sup> NaS				
30	320	$4.38 \pm 0.08$	$1.03 \pm 0.03$	0.999
40	315	$4.96 \pm 0.05$	$0.95 \pm 0.02$	0.999
45	314	$4.50 \pm 0.01$	$0.96 \pm 0.01$	0.999
53	314	$3.39 \pm 0.01$	$0.34 \pm 0.01$	0.999

and “dynamic” percolation, the experimental values may not always comply with this. According to the effective medium theory (EMT), the equation of Böttcher<sup>45</sup> is equivalent in form with the scaling law for  $\phi_d^t = 0.33$  and  $m = 1$  so that

$$\sigma = 1.5\sigma_d(\phi_d - 0.33) \quad (2)$$

where  $\sigma_d$  is the specific conductance of the dispersed phase and  $1.5\sigma_d = k$ .

The  $m$  and  $k$  for the microemulsion systems were obtained from the slope and intercept, respectively, of the  $\ln \sigma$  vs  $\ln(\phi_d - \phi_d^t)$  plot by a linear least-squares fitting procedure. The values are given in Table 2 along with correlation coefficients and errors in the slope and intercept. The values of  $\ln k$  and  $m$  fall in the range of 9.66–16.20 and 0.67–2.62, respectively. The experimental values of  $m$  thus lie on both sides of the predicted value<sup>9,16,30</sup> of 1.9. The results obtained in our earlier work and reported by other workers also deviated from 1.9.

For the temperature-induced percolation in w/o microemulsion at a constant  $\omega$ , the scaling law has the form<sup>27–30</sup>

$$\sigma = P(\theta - \theta_t)^n \quad (3)$$

where  $\theta$  is the temperature corresponding to the specific

conductance  $\sigma$ ,  $\theta_t$  is the threshold temperature,  $n$  is an exponent, and  $P$  is a constant.  $\theta_t$  was evaluated from the differential plot of  $(\delta \ln \sigma / \delta \theta)$  vs  $\theta$  similar to that used for obtaining  $\phi_d^t$  in water-induced percolation. The graphical plot of  $\ln \sigma$  vs  $\ln(\theta - \theta_t)$  was then processed by least-squares analysis, and  $n$  and  $\ln P$  were obtained from the slope and the intercept, respectively. The results with error limits are presented in Table 3. The experimental values of  $n$  fall in the range of 0.34–1.56; all the values are appreciably less than the expected value of 1.9.<sup>9,16,30</sup> The  $\ln P$  values are obtained in the range of 2.2–6.54.

The above results support the forms of scaling equations but not in terms of their constants and exponents. Similar observations were also made by us on AOT-containing microemulsion systems both with and without additives.<sup>33,34</sup> This difference is considered to arise from the physical difference between microdispersions of water droplets in an oil continuum and the mixed systems of conductors and insulators.<sup>46,47</sup> In the static percolation model, conducting ensembles are randomly embedded in an insulating matrix and the conductivity vanishes below the percolation threshold,<sup>48</sup> whereas in the dynamic model, the clusters in microemulsion continuously rearrange themselves by Brownian motion with a resultant conductance even below the threshold.<sup>15</sup> Near the critical region, the motion of water globules and rearrangement of clusters may undergo a transition to large and well-connected clustered droplets as a matrix of charge carrier. Recent NMR self-diffusion and conductivity measurements have established the motion of counterions via water channels within the droplet clusters both below and above the percolation threshold; the “hopping” of ions may contribute minimally to the conductance in the latter stage.<sup>39</sup> The additives are considered to affect the cluster rearrangement and charge transport to alter both the percolation threshold and the scaling exponents. Probable mechanisms for the specific effects of NaC and NaS have been reported.<sup>19,33,34</sup> To resolve the matter, further detailed experimental exploration of this area under varied conditions is wanted.

#### Energetics of Droplet Clustering Leading to Percolation.

Recently, Moulik and Ray<sup>40</sup> and Ray et al.<sup>33,34</sup> have reported the thermodynamics of clustering of droplets in w/o microemulsions considering the clustered droplets as a different phase (pseudophase, like micelles). This concept has been subsequently considered by Ajith and Rakshit<sup>41</sup> and also by Alexandradis et al.<sup>42</sup> for the estimation of energetics of clustering of different w/o microemulsion systems.

The standard free energy of clustering ( $\Delta G_{cl}^\circ$ ) is obtained from the relation

$$(\Delta G_{cl}^\circ) = RT \ln X_d \quad (4)$$

where  $X_d$  is the mole fraction of the droplets and other terms have their usual significance.

The Gibbs–Helmholtz equation provides the standard enthalpy of clustering,

$$\frac{d(\Delta G_{cl}^\circ)/T}{d(1/T)} = \Delta H_{cl}^\circ \quad (5)$$

A representative plot is shown in Figure 4.

The use of  $\Delta G_{cl}^\circ$  and  $\Delta H_{cl}^\circ$  in the Gibbs equation then yields the entropy of clustering,  $\Delta S_{cl}^\circ$

$$\Delta S_{cl}^\circ = (\Delta H_{cl}^\circ - \Delta G_{cl}^\circ)/T \quad (6)$$

The energetic parameters of droplet clustering with and without additives (NaC and NaS) at four different  $\omega$  values (30,

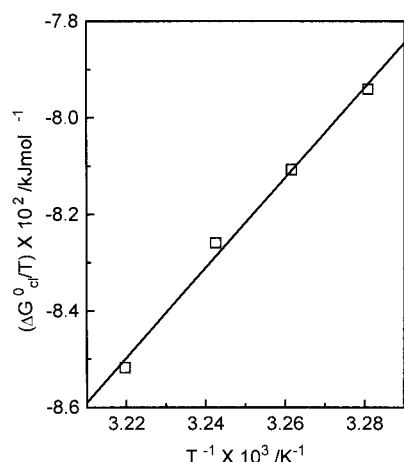


**Figure 4.** Representative  $-\Delta G^\circ_{\text{cl}}/T$  vs  $T^{-1}$  plot for the determination of  $\Delta H^\circ_{\text{cl}}$  of percolation for  $\text{H}_2\text{O}/\text{AOT}/n$ -heptane microemulsion system [composition:  $\text{H}_2\text{O}/\text{AOT}/n$ -heptane 1:0.63:2.28 (w/w);  $\omega = 39.52$ ].

**TABLE 4: Energetic Parameters for Droplet Clustering in the Water/AOT/*n*-Heptane w/o Microemulsion in the Absence and Presence of Additives**

	No Additive			
$\omega$	30	35	40	45
$\theta_t/k$	313	310	306	305
$[\text{droplet}] \times 10^4/\text{mol dm}^{-3}$	5.01	3.56	2.88	1.94
$-\Delta G^\circ_{\text{cl}}/\text{kJ mol}^{-1}$	27.0	27.8	24.2	
$\Delta H^\circ_{\text{cl}}/\text{kJ mol}^{-1}$	22.0	25.0	93.8	101
$\Delta S^\circ_{\text{cl}}/\text{J K}^{-1} \text{mol}^{-1}$	156	170	387	424
$E_p/\text{kJ mol}^{-1}$	341	486	740	307
	With 1.0 m mol $\text{dm}^{-3}$ NaS			
$\omega$	30	40	45	53
$\theta_t/K$	318	312	308	310
$[\text{droplet}] \times 10^4/\text{mol dm}^{-3}$	4.02	1.81	1.35	0.37
$-\Delta G^\circ_{\text{cl}}/\text{kJ mol}^{-1}$	27.7	29.3	29.9	32.4
$\Delta H^\circ_{\text{cl}}/\text{kJ mol}^{-1}$	15.1	44.2	54.0	61.0
$\Delta S^\circ_{\text{cl}}/\text{J K}^{-1} \text{mol}^{-1}$	133	236	271	302
$E_p/\text{kJ mol}^{-1}$	864	532	521	618
	With 0.1 mol $\text{dm}^{-3}$ NaC			
$\omega$	25	30	35	40
$\theta_t/k$	295	291	288	285
$[\text{droplet}] \times 10^4/\text{mol dm}^{-3}$	7.47	4.12	2.18	1.68
$-\Delta G^\circ_{\text{cl}}/\text{kJ mol}^{-1}$	24.2	25.3	26.4	26.8
$\Delta H^\circ_{\text{cl}}/\text{kJ mol}^{-1}$	24.0	29.4	41.3	115
$\Delta S^\circ_{\text{cl}}/\text{J K}^{-1} \text{mol}^{-1}$	164	188	235	498
$E_p/\text{kJ mol}^{-1}$	438	434	525	669

35, 40, and 45) are presented in Table 4.  $\theta_t$  has rightly increased with lowering of droplet concentration at each  $\omega$ . The positive  $\Delta H^\circ_{\text{cl}}$  and  $\Delta S^\circ_{\text{cl}}$  have both increased with  $\omega$ . The values of the  $\Delta S^\circ_{\text{cl}}$  are high and are very nearly the same at a fixed  $\omega$  (the tabulated single value of  $\Delta S^\circ_{\text{cl}}$  thus stands for all four compositions). At a comparable  $\omega$ , both the  $\Delta H^\circ_{\text{cl}}$  and  $\Delta S^\circ_{\text{cl}}$  follow the order NaS (1.0 m mol  $\text{dm}^{-3}$ ) < without additive < NaC (0.1 mol  $\text{dm}^{-3}$ ). The endothermicity of the clustering process accounts for a strong heat absorbing step in it. The clustering phenomenon is essentially a combination of two processes: (1) removal of the oil barrier enclosing the nanodroplets in the oil continuum and (2) association of the isolated droplets. The first process is endothermic, and the second is exothermic. The algebraic sum of the two is the measured enthalpic quantity. The first process, therefore, wins over the second. In the first process, the solvent surrounding the droplet microenvironment is disrupted and more than compensates for their association in the form of clusters manifesting an overall positive entropy change. It parallels the energetics of micellization (usually an endothermic process) where the entropy changes are normally positive.<sup>49</sup> The lower positive enthalpy change in the presence

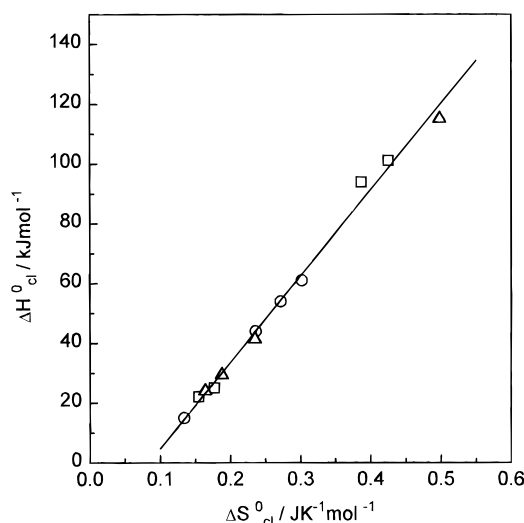


**Figure 5.** Enthalpy ( $\Delta H^\circ_{\text{cl}}$ ) – entropy ( $\Delta S^\circ_{\text{cl}}$ ) compensation plot for clustering of  $\text{H}_2\text{O}/\text{AOT}/n$ -heptane w/o microemulsion system at 303 K: (○) no additive; (△) 0.1 mol  $\text{dm}^{-3}$  NaC; (□) 1.0 m mol  $\text{dm}^{-3}$  NaS. Compensation temperature = 289 K.

of additive NaS than in its absence means there is a relatively less organized, i.e., easily disruptable, microsurrrounding of the droplets. With NaC, the environment is relatively more organized, requiring higher absorption of heat for interdroplet interaction. Once they are close, the phenomenon of percolation efficiently occurs by a special bridging mechanism proposed earlier.<sup>33</sup> The variation of  $\Delta G^\circ_{\text{cl}}$  in a narrow range has advocated linear compensation between  $\Delta H^\circ_{\text{cl}}$  and  $\Delta S^\circ_{\text{cl}}$  whose least-squares plot is illustrated in Figure 5 yielding a fitting relation (eq 7) with a correlation coefficient of 0.997,

$$\Delta H^\circ_{\text{cl}} = -24.21 + 289\Delta S^\circ_{\text{cl}} \quad (7)$$

The high values of  $\Delta S^\circ_{\text{cl}}$  mean that, like micelle formation, the clustering process is entropy controlled. Apparently, a clustering (or association) process is expected to end up with negative entropy change. This may not be a rule if an associated process (as disruption of the oil barrier herein considered) involves disorder in the system. It is known that the process of amphiphile association leading to micellization results in a positive entropy change since during transfer of the amphiphile into the micelle the “iceberg” surrounding the nonpolar tail melts, which is a considerable disorder-producing phenomenon in the system. The droplet-clustering phenomenon has thus basic parallelism with the amphiphile self-aggregation process. An explanation along a similar line has also been proposed earlier by us and by Alexandradis et al.<sup>42</sup> and Nazzario et al.<sup>36</sup> Further work using amphiphiles differing in nonpolar tails as well as headgroups is required to shed more light on the matter of energetics of the clustering process.

The  $\Delta H^\circ_{\text{cl}}$  values are profiled with  $\omega$  in Figure 6. A sigmoidal dependence is envisaged, indicating a sizable  $\Delta H^\circ_{\text{cl}}$  change at  $\omega \approx 35$ . The phenomenon is mild in the presence of NaS; in the presence of NaC, the phenomenon is to some extent more efficient than that without additive. At constant temperature, the clustering process is more spontaneous with increasing  $\omega$ , i.e., with increasing droplet size. Similar to  $\Delta H^\circ_{\text{cl}}$ ,  $\Delta S^\circ_{\text{cl}}$  has also increased with  $\omega$ . After a threshold  $\omega$  (or droplet dimension), there is a rapid change in the involved energetics of the process. The total scenario depends on a number of factors, viz., the droplet number and size, the interface, the nature of the continuum, the presence of additive, the temperature, etc. The

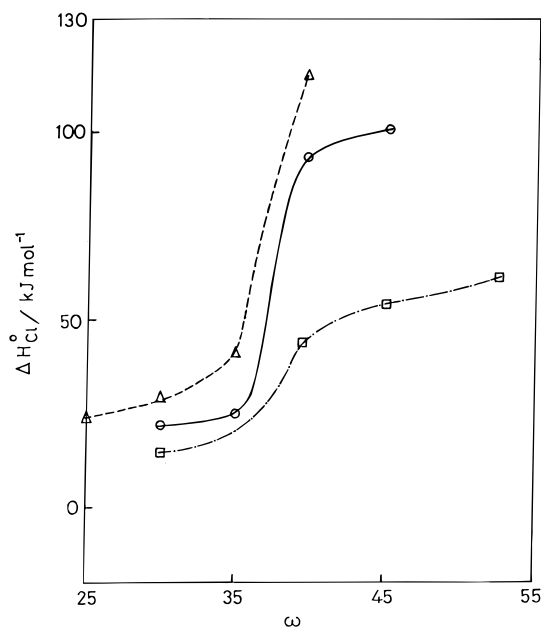


**Figure 6.**  $\Delta H^\circ_{cl}$  vs  $\omega$  profile for  $H_2O/AOT/n$ -heptane w/o microemulsion system in the presence and absence of additives at 303 K: (O) no additive; ( $\Delta$ )  $0.1 \text{ mol dm}^{-3}$  NaC; ( $\square$ )  $1.0 \text{ mol dm}^{-3}$  NaS.

contributions of all these factors make the process complex enough but worthy of further intimate investigation.

**Activation Energy of Percolation.** The activation energy ( $E_p$ ) for conductance in the postpercolation stage has been estimated on the basis of an Arrhenius form of relation and by plotting  $\ln \sigma$  vs  $T^{-1}$

$$\sigma = A e^{-E_p/RT} \quad (8)$$

where  $A$  is a constant,  $\sigma$  is the conductance, and  $R$  and  $T$  have their usual significance.

The  $E_p$  values are also given in Table 4. The  $E_p$  values for percolating microemulsion systems have been also reported in the past.<sup>20,32,34</sup> They can be low and high for weak<sup>32</sup> and strong<sup>20,34</sup> percolating systems, respectively. They do not strictly follow a trend;  $E_p$  may either increase or decrease with  $\omega$ , and they may also pass through a maximum. Additives may have specific effects on  $E_p$ . The phenomenon of percolation is different than normal conductance, and the special effect of enhancement of conductance is expected to cross (or overcome) a large barrier requiring a large energy of activation. Large  $E_p$  values have also been earlier realized.<sup>20,34</sup> It has been observed in the present study that, in the absence of additive,  $E_p$  has shown a tendency to pass through a maximum with respect to  $\omega$ , whereas in the presence of NaC and NaS, the  $E_p$  has shown a declining trend.

**Dimension and Diffusion of Nanodroplets.** The hydrodynamic diameter of nanodroplets of water ( $d_h$ ), their diffusion coefficient ( $D$ ), and the polydispersity index (PDI) were measured in terms of  $\omega$  by the DLS method. The droplet size distribution at and before percolation without additive is illustrated in Figure 7. The results are presented in Figure 8. The diameter has been found to mildly increase up to  $\omega \approx 15$ , and there is a discontinuity (sudden depression) in the range of  $\omega$  between  $\sim 20$ – $32$ ; thereafter, the size increases rapidly. The trend roughly corroborates (in the lower range of  $\omega$ ) the theoretical line  $T$  drawn on the basis of the formula<sup>44</sup> for the hydrodynamic diameter ( $d_h$ ),

$$d_h = 2(0.13\omega + 1.185) \quad (9)$$

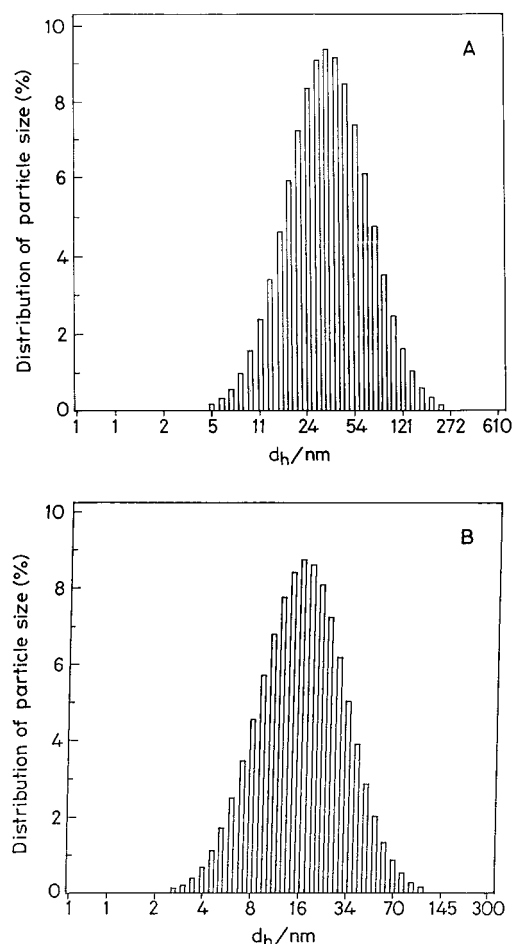


**Figure 7.** Droplet size distribution of  $H_2O/AOT/n$ -heptane system determined by DLS method at (A) and before (B) percolation: (A)  $\omega = 39.52$ ;  $T = 308.9 \text{ K}$  ( $\theta_i = 308.5 \text{ K}$ ); (B)  $\omega = 39.52$ ;  $T = 303 \text{ K}$ .

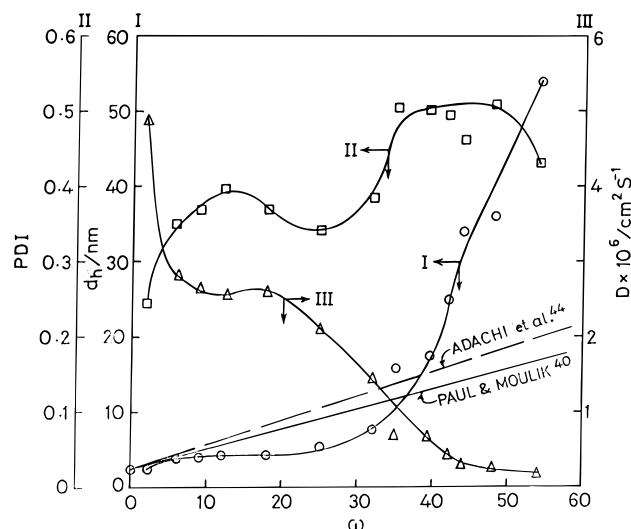


**Figure 8.** The  $d_h$ , PDI, and  $D$  profiles with  $\omega$  for  $H_2O/AOT/n$ -heptane w/o microemulsion system at 303 K. Ordinate scales are shown on the curves.

Similar equations were also proposed earlier by Adachi et al.,<sup>50</sup> Nicholson and Clarke,<sup>51</sup> and Pileni.<sup>52</sup>

The departure in the size beyond  $\omega = 40$  is significantly large. Similar dependence of hydrodynamic radius ( $r_h$ ) on  $\omega$  at constant [oil]/[AOT] ratio has been observed by Nazzario et al.<sup>36</sup> The  $r_h$  values at infinite dilution have also shown identical dependence; the deviation from the expected linear course is not due to

**TABLE 5: Hydrodynamic Diameter ( $d_h$ ), Polydispersity Index (PDI), and Diffusion Coefficient ( $D$ ) of H<sub>2</sub>O/AOT/Heptane w/o Microemulsion ( $\omega = 39.52$ ) at Different Thermal Conditions in the Presence and Absence of NaS and NaC**

temp/K	$d_h$ /nm	PDI	$D \times 10^7/\text{cm}^2 \text{S}^{-1}$
No Additive			
300	13.6	0.553	8.40
309	26.6	0.605	4.42
313 <sup>a</sup>	1362	2.380	0.087
With 1.0 m mol dm <sup>-3</sup> NaS			
302	51.7	0.605	2.22
308	62.6	0.691	1.87
311 <sup>a</sup>	1109	1.765	0.121
324 <sup>a</sup>	2364	3.881	0.052
With 0.1 mol. dm <sup>-3</sup> NaC			
280	62.3	0.591	1.70
283	62.7	0.601	1.72
285	43.4	0.664	2.08
292	24.0	0.517	3.86
299	24.7	0.500	4.60
314 <sup>a</sup>	336	0.404	0.369

<sup>a</sup> Phase separation.

micellar attractive interaction. The discontinuity at  $\omega \approx 30$  has been rationalized due to refractive index matching composition, i.e., the refractive index of the dispersed phase is equal to that of the oil (isooctane). Following the models<sup>53</sup> that relate the refractive index with  $\omega$ , for water/AOT/isooctane system, the index matching point has been found<sup>36</sup> to be at  $\omega = 30.9$  in close agreement with the experimental value of 30. The point of maximum deviation for the presently studied system of water/AOT/heptane at  $\omega \approx 28$  can be taken to be in conformity with the index matching rationale because of comparable refractive indices of heptane and isooctane (1.387 and 1.391, respectively, at 20 °C). The sharp rise at  $\omega > 40$  can be due to clustering, shape fluctuation, as well as polydispersity. For bigger droplets (i.e., at higher  $\omega$ ), the interface tends to flatten with possible fluctuation of shape. But interdependence between droplet size and polydispersity has a trend up to  $\omega = 40$ ; the polydispersity (PDI) has been found to be directly dependent on  $d_h$ . For dispersions with  $\omega > 40$ ,  $d_h$  rises rapidly whereas PDI tends to level off. This can be reasoned out by way of clustering of droplets on the higher side of  $\omega$  than 40. The diffusion coefficient ( $D$ ) is inversely dependent on  $d_h$ . It is very sensitive on the lower side of  $\omega$ ; there is a halt at  $\omega \approx 18$ , thereafter,  $D$  sharply decreases up to  $\omega = 40$  and finally tends to level off. The PDI and  $D$  values are inversely related. The “crest” and “trough” positions of PDI more or less match with the “trough” and “crest” positions of  $D$ . The large changes in PDI and  $D$  with mild changes in  $d_h$  for the dispersions with  $\omega < 20$  demands a special effect for rationalization. Ruling out attractive interaction in the lower range of  $\omega$  in line with the report of Nazzario et al.,<sup>36</sup> the above phenomenon is intriguing.

In Table 5, the  $d_h$ ,  $D$ , and PDI of the percolating water/AOT/heptane system at different temperatures with and without additives are presented at a constant  $\omega = 39.5$ . In the absence of additive, the diameter becomes enormously large above  $\theta_t$ , the scattering center becomes very large corresponding to a state of infinite cluster formation. At higher temperature, shape fluctuation and clustering can lead to much increased droplet size. The corresponding PDI and  $D$  values are consequences of this effect. The diameter increases in the presence of NaS, and the tendency of infinite cluster formation above  $\theta_t$  also prevails in the system. In the presence of NaC, the size is initially greater than the other two cases, which declines at the percolation threshold (284.5 K), there is a nearly 13-fold increase in the

size. The  $D$  and PDI values also vary correlatively with the  $d_h$  values of the preparations. Increased droplet size in the percolation range of the water/AOT/isooctane system has been reported by Nazzario et al.;<sup>36</sup> they of course did not observe very large scattering units in their system. We have observed that, at the point of phase separation, the scattering centers become enormously large. The size (13.6 nm) of the droplets without additive (Table 5) at 300 K (below the threshold temperature of 308.4 K) moderately agrees with the calculated value (15.1 nm) according to the formula given in eq 9. We conclude that in the early part of the percolation temperature the size variation is not drastic; the droplets make more contacts but retain their individual identities. In the presence of NaS, the effective size of the droplets is much greater than that calculated, but a large increase takes place just after  $\theta_t$ . In the presence of NaC, the droplet size is larger than expected, but it progressively decreases with increasing temperature past  $\theta_t$  until a temperature difference of 29° is reached. The tendency of the droplets to retain their individual identity in the cluster is not envisaged. The large change in  $d_h$  at temperatures reasonably higher than  $\theta_t$  may be also due to shape fluctuation. A reasonably detailed study of the effects of the additives, viz., alkanols and alkyl polyoxyethylene ethers (with increasing headgroups) has been made by Nazzario et al.<sup>36</sup> In their opinion, the alkanols reduce shape fluctuations and the  $r_h$  values are less than that in the absence of the alkanols. The polyoxyethylene alkyl ethers impart increased  $r_h$  with increasing headgroup size; by their presence, these additives help fluctuation of shape, which manifests in larger  $r_h$  by the DLS method. This may also lead to phase separation. The effects of the additives NaS and NaC to increase  $d_h$  (NaC is more effective than NaS, at temperatures less than  $\theta_t$ , in this respect) of the droplets of the system herein reported may have a component of fluctuation in shape. Until further detailed studies using additives of different kinds are done, the final say on the matter remains pending.

## Conclusions

- (1) The water/AOT/*n*-heptane system produces large monophasic zones in the presence and absence of NaC and NaS over a wide range of temperature.
- (2) The percolation of conductance of the microemulsion system is assisted by NaC and retarded by NaS.
- (3) The results fit in the scaling equations, but constants and exponents are different from expectations.
- (4) The droplet clustering process is endothermic, and the associated entropy change is positive.
- (5) In the percolation region, on the whole, the droplets maintain their individual geometrical identities in the absence of NaC and NaS.

**Acknowledgment.** Financial assistance from Department of Science and Technology, Government of India, is gratefully acknowledged.

## References and Notes

- (1) *Microemulsions*; Robb, I. D., Ed.; Plenum Press: New York, 1982.
- (2) Bothorel, P. *Microemulsions*, *Cour. CNRS* **1982**, 48, 39.
- (3) Paul, B. K.; Moulik, S. P. *J. Dispersion Sci. Technol.* **1997**, 18, 301.
- (4) Moulik, S. P.; Pal, B. K. *Adv. Colloid Interface Sci.* **1998**, 78, 99.
- (5) Kunieda, H.; Asaoka, H.; Shinoda, K. *J. Phys. Chem.* **1988**, 92, 185.
- (6) *Microemulsions: Theory and Practice*; Prince, L. M., Ed.; Academic Press: New York, 1977.



- (7) Eicke, H. F.; Brokovic, M.; Dasgupta, B. *J. Phys. Chem.* **1989**, 93, 314.
- (8) Jada, A.; Lang, J.; Zana, R.; Makhlouff, R.; Hirsch, E.; Candau, S. O. *J. Phys. Chem.* **1994**, 94, 387.
- (9) Moha-Ouchane, M.; Peyrelasse, J.; Boned, C. *Phys. Rev. A* **1987**, 35, 3027.
- (10) Safran, S. A.; Webman, I.; Grest, G. S. *Phys. Rev. A* **1985**, 32, 506.
- (11) Bug, A. L. R.; Safran, S. A.; Grest, G. S.; Webman, I. *Phys. Rev. Lett.* **1985**, 55, 1896.
- (12) Safran, S. A.; Grest, G. S.; Bug, A. L. R. In *Microemulsion Systems*; Rosano, H. L., Clause, M., Eds.; Marcel Dekker, Inc.: New York, 1987; p 235.
- (13) Lagues, M.; Santerey, C. *J. Phys. Chem.* **1980**, 84, 3503.
- (14) Hilfiker, R.; Eicke, H. F.; Geiger, S.; Furlur, G. *J. Colloid Interface Sci.* **1985**, 105, 378.
- (15) Grest, G. S.; Webman, I.; Safran, S. A.; Bug, A. L. R. *Phys. Rev. A* **1986**, 33, 2842.
- (16) Peyrelasse, J.; Moha-Ouchane, M.; Boned, C. *Phys. Rev. A* **1988**, 38, 904.
- (17) Maitra, A. N.; Mathew, C.; Varshney, M. *J. Phys. Chem.* **1990**, 94, 5290.
- (18) Jada, A.; Lang, J.; Zana, R. *J. Phys. Chem.* **1989**, 93, 10.
- (19) Dutkiewicz, E.; Robinson, B. H. *J. Electroanal. Chem.* **1988**, 251, 11.
- (20) Mukhopadhyay, L.; Bhattacharya, P. K.; Moulik, S. P. *Colloids Surf.* **1990**, 50, 295.
- (21) Bisal, S. R.; Bhattacharya, P. K.; Moulik, S. P. *J. Phys. Chem.* **1990**, 94, 530.
- (22) Brokovic, M.; Eicke, H. F.; Hammerich, H.; Dasgupta, B. *J. Phys. Chem.* **1985**, 92, 206.
- (23) Jada, A.; Lang, J.; Candau, S. J.; Zana, R. *Colloids Surf.* **1989**, 38, 251.
- (24) Bisal, S. R.; Bhattacharya, P. K.; Moulik, S. P. *J. Surf. Sci. Technol.* **1988**, 4, 121.
- (25) Lagues, M. *J. Phys. Lett. (Fr.)* **1979**, L-33, 40.
- (26) Peyrelasse, J.; Boned, C. *Phys. Rev. A* **1990**, 41, 938.
- (27) Lagourette, B.; Peyrelasse, J.; Boned, C.; Clause, M. *Nature (London)* **1979**, 281, 60.
- (28) Lagues, M.; Ober, R.; Taupin, C. *J. Phys. Lett. (Paris)* **1978**, L39, 487.
- (29) Ray, S.; Bisal, S. R.; Moulik, S. P. *Proceedings of the National Conference on Physical and Chemical Aspects of Organized Biological Assemblies*; Indian Society for Surface Science and Technology: Jadavpur University, Calcutta, India, 1991; pp 85–89.
- (30) Feldman, Y.; Korlovich, N.; Nir, L.; Garti, N. *Phys. Rev. E* **1995**, 51, 478.
- (31) Mitescu, C. D.; Mulsoff, M. J. *J. Phys. Lett. (Paris)* **1983**, L-679.
- (32) Mukhopadhyay, L.; Bhattacharya, P. K.; Moulik, S. P. *Ind. J. Chem.* **1993**, 32A, 485.
- (33) Ray, S.; Bisal, S. R.; Moulik, S. P. *J. Chem. Soc., Faraday Trans.* **1993**, 89, 3277.
- (34) Ray, S.; Paul, S.; Moulik, S. P. *J. Colloid Interface Sci.* **1996**, 183, 6.
- (35) Garcia-Rio, L.; Leis, J. R.; Mejuto, S. C.; Pena, M. E. *Langmuir* **1994**, 10, 1976.
- (36) Nazzario, L. M. M.; Hatton, T. A.; Crespo, J. P. S. G. *Langmuir* **1996**, 12, 6326.
- (37) Garcia-Rio, E.; Herves, P.; Leis, J. R.; Mejuto, J. C. *Langmuir*, in press.
- (38) Hurugen, J. P.; Authier, M.; Greffe, J. L.; Pileni, M. P. *Langmuir* **1991**, 7, 243.
- (39) Feldman, Y.; Kozlovich, N.; Nir, I.; Garti, N.; Archipov, V.; Idiyatullin, Z.; Zuev, Y.; Fedtov, V. *J. Phys. Chem.* **1996**, 100, 3745.
- (40) Moulik, S. P.; Ray, S. *Pure Appl. Chem.* **1994**, 66, 521.
- (41) Ajith, S.; Rakshit, A. K. *J. Phys. Chem.* **1995**, 99, 14778.
- (42) Alexandridis, P.; Holzwarth, J. F.; Hatton, T. A. *J. Phys. Chem.* **1995**, 99, 8222.
- (43) Kar, P.; Moulik, S. P. *Ind. J. Chem.* **1995**, 34A, 700.
- (44) Paul, S.; Moulik, S. P. *Tenside, Surfactants, Deterg.* **1995**, 6, 32 and discussion therein.
- (45) Böttcher, C. J. F. *Recl. Trav. Chem.* **1945**, 64, 47.
- (46) Bernasconi, J.; Wiesmann, J. *Phys. Rev. B: Condens. Matter* **1976**, 13, 1131.
- (47) Granqvist, C. G.; Hunderi, O. *Phys. Rev. B: Condens. Matter* **1978**, 18, 1554.
- (48) Kirkpatrick, S. *Rev. Mod. Phys.* **1973**, 45, 574.
- (49) Shaw, J. *Introduction to Colloid and Surface Chemistry*, 3rd ed.; Butterworths: Markham, ON, Canada, 1980; pp 85–87.
- (50) Adachi, M.; Harada, M.; Shioi, A.; Sato, Y. *J. Phys. Chem.* **1991**, 95, 7925.
- (51) Nicholson, J. D.; Clarke, J. H. R. In *Surfactants in Solution*; Mittal, K. R., Lindman, B., Eds.; Plenum Press: New York, 1984; p 1663.
- (52) Pileni, M. P. In *Structure and Reactivity in Reversed Micelles*; Pileni, M. P., Ed.; Elsevier: Amsterdam, 1989.
- (53) Ricka, J.; Borkovec, M.; Hofmeir, U. *J. Chem. Phys.* **1991**, 94, 8503.
- Alexandridis, P.; Holzwarth, J. F.; Hatton, T. A. *Langmuir* **1993**, 9, 2045.